The 19th Cambridge Workshop on Cool Stars, Stellar Systems, and the Sun
Edited by G. A. Feiden

Li-rich AGB/RGB stars: Lithium abundances and mass loss

Walter J. Maciel, Roberto D. D. Costa

Astronomy Department, University of São Paulo, São Paulo, Brazil

Abstract

Most metal-rich AGB/RGB stars present strong Li underabundances, since this element is easily destroyed in the high temperatures of the stellar interiors. In spite of this fact, several of these stars are Li-rich, having Li abundances given by ϵ(Li) = log (Li/H)+12 $>$ 1.5. In a previous work we have shown that high-metallicity Li-rich stars follow the same average Li abundance trend with metallicity as the metal-poor stars, although with a larger dispersion. More recently, we have investigated the existence of correlations of the Li abundances with several physical properties of the stars, such as the effective temperature, mass, radius, and luminosity. In the present work, we extend this investigation to the expected mass loss rates of these stars. Specifically, we look for correlations between the Li abundances and the mass loss rates or related parameters in Li-rich AGB/RGB stars. We have estimated the mass loss rates using a modified form of the Reimers formula and applied it to a large sample of 104 Li-rich giant stars for which reliable stellar data are available. Our proposed method assumes a linear relation between the stellar luminosity and the Li abundance, so that the luminosity can be estimated from the Li abundance. The stellar mass is then obtained from the effective temperature and luminosity using recent evolutionary tracks. The stellar radius can be determined from the stellar gravity, so that the mass loss rate can be calculated using an adequate calibration involving both Li-rich and Li-poor stars in the AGB/RGB branches. The results show that most Li-rich stars have lower mass loss rates compared with C-rich or O-rich giants that do not present Li enhancements.

1 Introduction

Most metal-rich AGB/RGB stars present strong Li underabundances, since this element is easily destroyed in the high temperatures of the stellar interiors. However, several of these stars are Li-rich, with Li abundances by number of atoms given by ϵ(Li) = log (Li/H) + 12 $>$ 1.5. Li-rich giant stars comprise low mass stars in the Red Giant Branch (RGB), especially those located at the luminosity bump, and intermediate mass stars in the Asymptotic Giant Branch (AGB), especially those near the giant branch clump. The main production mechanism for ^{7}Li is believed to be the Cameron-Fowler mechanism (Cameron and Fowler 1971), in which there is an enrichment of ^{3}He following the first dredge-up episode. The excess ^{3}He may reach the inner stellar layers, where it is burned to form ^{7}Be, which leads to the production of ^{7}Li. This element is then raised to the stellar outer layers, which characterizes the Li-rich phase, before being burned out or diluted into the stellar atmosphere.

In a previous work we have considered a large sample of Li-rich stars, and investigated the Li abundance trends with several stellar parameters, such as metallicity, the effective temperature, mass, radius, and luminosity (Maciel & Costa 2012, 2015). In the present work, we apply the correlations involving the stellar radius and luminosity with the Li abundance and look for correlations between the abundances and the mass loss rates or related parameters in Li-rich AGB/RGB stars. Comparing these results with data from Li-poor stars for which luminosities and mass loss rates are independently known, we derive the mass loss rates of Li-rich RGB/AGB stars. Section 2 discusses in detail the Li-rich and L-poor stellar samples considered, section 3 describes the adopted method, and section 4 presents the results obtained so far.

2 The Sample

2.1 Li-rich stars

The initial sample of Li-rich AGB/RGB stars is the one previously considered by Maciel & Costa (2012, 2015), with seven additional stars from Brown et al. (1989). As discussed in more detail by Maciel & Costa (2012, 2015), the original sources of the data are Brown et al. (1989), Mallik (1999), Gonzalez et al. (2009), Monaco et al. (2011), and Kumar et al. (2011). This sample was extended by the inclusion of several Li-rich stars recently published, as given by Lebzelter et al. (2012), Monaco et al. (2014), Kövári et al. (2013), Martell & Shetrone (2013), and Lyubimkov et al. (2012).

Lebzelter et al. (2012) derived spectroscopic Li abundances in a sample of bulge stars from the bottom to the tip of the red giant branch. It is known that a few giants on the ascending RGB are Li-rich, as well as some stars at the bump of the luminosity function on the RGB for low mass stars and on the AGB for intermediate mass stars. The authors have used FLAMES spectra along with COMARCS atmospheres and bulge giant isochrones and derived effective temperatures, gravities and Li abundances from the 670.8 nm Li line. From an original sample of 401 stars, Lebzelter et al. (2012) have found detectable Li 670.8 nm line in 31 stars, and 3 of them can be considered as Li-rich using the criterium mentioned earlier. These stars are located on the upper RGB, above the luminosity bump.

Monaco et al. (2014) identified a super Li-rich star in the open cluster Trumpler 5 based on FLAMES/VLT spectra and 3D-NLTE models. The star is # 3416, which is a core He-burning red clump star with ϵ(Li) = 3.75. The star is located at α(2000) = 06:36:40.2 and δ(2000) = 09:29:47.8.

Kövári et al. (2013) presented Doppler imaging of two Li-rich K giants and used optical spectroscopy and photometry

to derive their fundamental properties, such as effective temperature, luminosities, masses, etc. From their analysis it is concluded that both stars are located at the end of the first Li dredge-up on the RGB.

Martell & Shetrone (2013) presented a sample of 23 Li-rich field giants from the Sloan Digital Sky Survey with high-resolution follow up spectroscopy. These objects are located in the upper right region of the HR diagram, including the RGB, the AGB and the red clump. For these objects, high resolution spectroscopy leads to the determination of the stellar parameters. The stellar masses are probably in the range 1–3 $M_{\odot}$, where the lower limit corresponds to stars in the RGB, particularly those near the luminosity bump, and the upper limit corresponds to AGB stars (cf. Charbonnel & Balachandran 2000).

Lyubimkov et al. (2012) derived accurate Li abundances in a sample of F, G giants and supergiants, out of which there are 15 objects having ϵ(Li) > 1.5, that is, are Li-rich according to the criterium adopted here.

As we will see in the next section, in order to apply our method, the effective temperature T_{eff} , gravity $\log g$, and Li abundance ϵ(Li) of the Li-rich stars must be known. Applying this condition and removing some objects that lie outside the range of the adopted parameters, namely the Li-abundance, luminosity and effective temperature, a final sample of 104 Li-rich stars is obtained For details on these stars, the reader is referred to the original papers.

2.2 Li-poor stars

There are reliable determinations of the luminosities and mass loss rates for many RGB/AGB stars without Li enhancements in the literature, which can be used in order to estimate the corresponding quantities of Li-rich stars. The Li-poor stars used as a comparison with the Li-rich objects come from the large samples by Gullieuszik et al. (2012) and Groenewegen et al. (2009).

Gullieuszik et al. (2012) obtained accurate mass loss rates and luminosities for a large sample of AGB stars in the LMC from the VISTA survey (VMC). Dust radiation transfer models were compared with the obtained spectral energy distributions (SED) from VMC data and available photometry from the optical to mid-infrared wavelengths. The AGB sample includes 373 objects. Excluding the objects for which the complete calculation could not be done by lack of data (mass loss rate dM/dt and/or luminosity $\log L/L_{\odot}$), we have a final sample of 178 objects.

Groenewegen et al. (2009) used dust radiative transfer models for a large sample of C-rich and O-rich AGB stars in the SMC and LMC with Spitzer data, and derived mass loss rates and luminosities for these objects. The O-rich stars were classified as foreground objects (FG), red supergiants (RSG) and AGB stars. The obtained relations involving the mass loss rates, luminosities and pulsation periods were further compared with predictions of models by Vassiliadis & Wood (1993) as well as models based on the Reimers mass loss relation. The total C-rich AGB star sample included 101 objects, but the object # 069 wbp17 has a mass loss rate several orders of magnitude below the other objects, so that it will be excluded, remaining 100 stars in the C-rich sample. The O-rich stars include 86 objects, but 10 stars are considered as foreground objects (FG) and about 42 objects considered as red supergiants (RSG), essentially based on the correlation between the bolometric magnitude and period derived by Wood et al. (1983). Excluding the FG and RSG objects we have 34 AGB stars in the O-rich sample. The Magellanic Clouds have the obvious advantage of a known distance, although their lower metallicity relative to the Milky Way may introduce some uncertainties when these relationships are applied to galactic objects. However, as discussed in Groenewegen et al. (2007), there is no clear evidence of a metallicity dependence of the mass loss rate for C-rich stars. The estimated uncertainties are generally of 10% for the luminosity and 25% in the mass loss rate. Groenewegen et al. (2009) give two sets of data, depending on the assumed dust composition. We have adopted the best overall fit, which corresponds to the first entry for each object in Table 4 of Groenewegen et al. (2009).

The sample of Li-poor stars include then 178 stars in the Gullieuszik sample, 100 stars in the C-rich sample by Groenewegen, and 34 stars in their O-rich sample, so that the total sample of Li-poor stars has 312 stars.

3 The Method

3.1 Empirical correlations of Li-rich stars

Maciel & Costa (2015) considered a large sample of Li-rich giant stars and investigated the existence of possible correlations involving the Li abundance and other stellar parameters. In the following we will consider two of these correlations, namely the correlations of the Li abundance with the stellar radius and luminosity.

In our previous work, a relation was obtained in the form $\epsilon(\mathrm{Li}) = f(R)$, as shown in Figure 1. In this figure, the empty circles are the Li-rich stars, the filled dots are average abundances taken in 2 $R_{\odot}$ bins and the dashed line shows a linear fit to the data, which is the simplest correlation, and can be considered as a first approximation. The corresponding equation can be written as

$$\epsilon(\mathrm{Li}) = a + b\ R/R_{\odot} \tag{1}$$

with $a = 2.30 \pm 0.11$, $b = 0.03 \pm 0.01$, and correlation coefficient $r = 0.81 \pm 0.20$. The correlation is assumed to be valid in the interval $0 \leq \log R/R_{\odot} \leq 30$ and $1.5 \leq \epsilon(\mathrm{Li}) \leq 4.0$.

From Figure 1, the Li abundance clearly seems to increase with the stellar radius, at least within a range that encompasses most the Li-rich stars in the sample. Explaining the origin of this correlation is a complex procedure, since the Li enrichment mechanism is not well known, and different models have been proposed for Li-rich giants near the luminosity bump, clump giants, and stars on the AGB branch. Some possibilities include incomplete Li dilution, hot bottom burning, cool bottom burning, among others. We have not addressed this aspect in detail, since our main goal here is to compare the mass loss rates of the Li-rich stars with the majority of Li-poor objects. However, some hints can be made, considering some recent models for the Li-enrichment in RGB/AGB stars. In particular, the recent work by Casey et al. (2016) based on 20 Li-rich giant stars from the Gaia-ESO survey explains the Li-enrichment process as a natural consequence of the engulfing of Jupiter-like planets, followed by deep mixing in the stellar envelope to produce additional Li. This is not proven yet, but in this case the Li-rich objects would favour larger stars, which present a larger cross section to absorb the planets, therefore leading to a $\epsilon(R)$ correla-

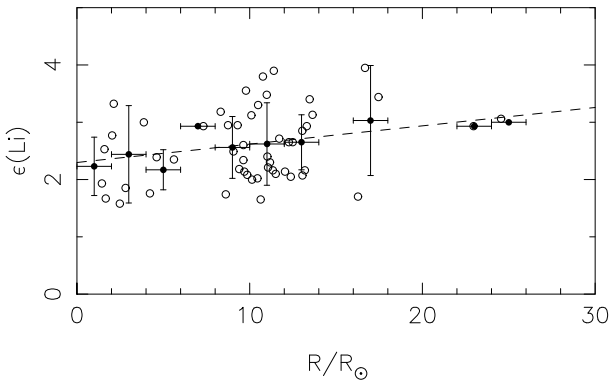

Figure 1: Correlation between the Li abundance and the stellar radius for Li-rich giant stars. The empty circles show the data used by Maciel and Costa (2015), and the black dots are average abundances in $2R_\odot$ bins. The dashed line shows the linear fit given by equation 1.

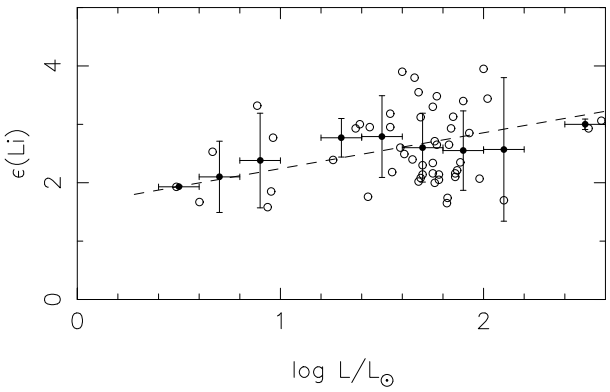

Figure 2: Correlation between the Li abundance and the stellar luminosity for Li-rich giant stars. The empty circles show the data used by Maciel and Costa (2015), and the black dots are average abundances in 0.2 dex luminosity bins. The dashed line shows the linear fit given by equation 2.

tion such as the one shown in Figure 1. A similar discussion along these lines was recently presented by Delgado Mena et al. (2016a, 2016b). Also, recently Kirby et al. (2016) proposed a scenario for Li enrichment involving mass transfer from Li-enriched companions to RGB stars, a procedure that will also favour larger stars, with an enhanced probability of absorbing the companions. As a conclusion, the observed relation is expected, at least on the basis of average values, as considered here.

Since we have $L \propto R^2\,T_{eff}^4$, the stellar luminosity is approximately proportional to the radius squared, as the effective temperature does not vary much in the considered sample. Therefore, one would then expect a correlation of the stellar luminosity and the Li abundance, which we have indeed obtained, as shown in Figure 2, which includes the data in the range $0 < \log L/L_\odot < 2.6$ as well as the averages in 9 luminosity bins. Analogously, for the Li abundances we have $1.5 \leq \epsilon(\mathrm{Li}) \leq 4$, but for stars near the lower limit very low luminosities are obtained, which are outside the range where calculations are possible, so that we adopt instead the range $1.8 \leq \epsilon(\mathrm{Li}) \leq 4.0$. The Li-rich phase is probably a short one in the life of a cool giant star, and our sample may include objects in different stages of Li enrichment, which can be seen from the scatter in Figure 2. However, an increase of the abundances with the luminosity is apparent, especially near the upper envelope, so that we feel safe in adopting an average relation between these quantities.

For practical purposes we will consider the inverse relation of the form $\log L/L_\odot = f[\epsilon(\mathrm{Li})]$, and the best correlation obtained for the average data is shown as a dashed line in Figure 2, which can be written as

$$\log L/L_\odot = c + d\,\epsilon(\mathrm{Li}) \qquad (2)$$

with $c = -2.65 \pm 1.07$, $d = 1.63 \pm 0.42$, and correlation coefficient $r = 0.83 \pm 0.43$. This equation is strictly valid in the luminosity interval $0 \leq \log L/L_\odot \leq 3.0$, but we have found that for the few objects with higher luminosities the results are essentially the same, so that a more flexible form of this range can be written as $0 \leq \log L/L_\odot \leq 5.0$. In fact, independent estimates of the luminosity of the Li-rich stars considered here are consistent with the adopted range. For example, from the bolometric magnitudes of the stars in the sample by Brown et al. (1989) we have $1.1 \leq \log L/L_\odot \leq 2.7$. Also, from the data by Mallik (1999), we get $0 \leq \log L/L_\odot \leq 3.0$.

3.2 Determination of the mass loss rates

We have developed several methods to estimate the mass loss rate of Li-rich AGB/RGB stars, based essentially on the Li-abundance and on some correlations as discussed previously by Maciel and Costa (2015). In the following we will present a method based on a modified form of the Reimers formula, and apply it to the Li-rich sample discussed in section 2. The method can be summarized as follows: we adopt the relation between the stellar luminosity and the Li abundance of Li-rich stars, as given by equation 2, so that the luminosity can be estimated from the Li abundance. The stellar mass is then obtained from the luminosity and effective temperature using recent evolutionary tracks. The stellar radius is determined from the stellar gravity, so that the mass loss rate can be calculated using an adequate calibration of the Reimers formula involving both Li-rich and Li-poor stars in the AGB/RGB branches. Therefore, the mass loss rate depends essentially on (i) the Li abundance ϵ(Li), (ii) the effective temperature T_{eff}, and (iii) the stellar gravity g.

As a first step, we determine the stellar luminosity using the relation between the luminosity and the Li abundance, as given by equation 2. It should be noted that using the relation between the Li abundance and the stellar radius given by equation 1 we obtain essentially the same results. Having the luminosity and the effective temperature, the mass can be estimated using recent evolutionary tracks for giant stars. We have adopted the tracks by Bertelli et al. (2008, see also Kumar et al. 2011). The tracks can be applied to solar metallicity stars with masses in the interval $1.0 < M/M_\odot < 3.0$, and effective temperatures in the range $3800 < T_{eff}(\mathrm{K}) < 5600$. The curves have been approximated by polynomials of order 3–6, and are shown in Figure 3. Since the effective temperature and luminosities are known and the tracks are reasonably detached, the determination of the stellar mass is a straighforward procedure.

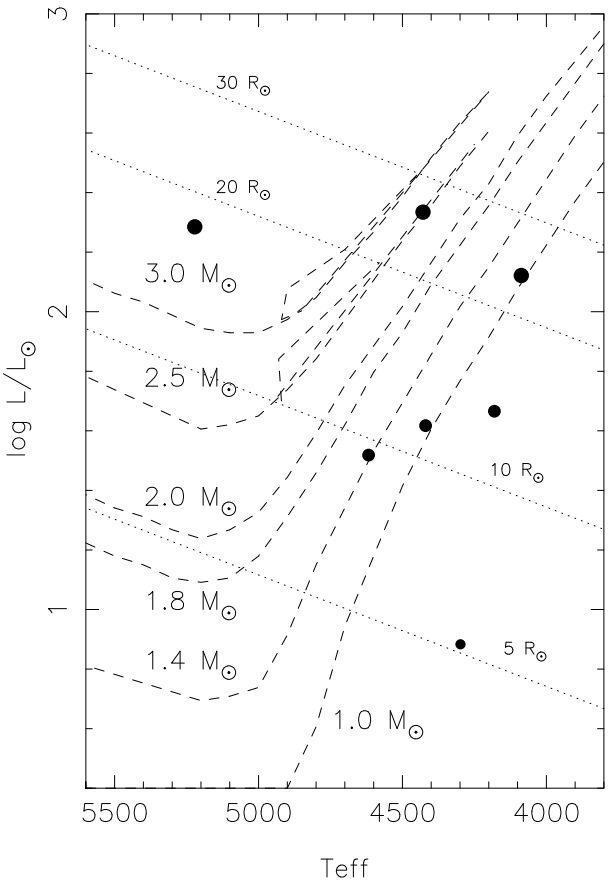

Figure 3: Adopted evolutionary tracks from Bertelli et al. (2008) for stars in the mass range $1.0 - 3.0\,M_{\odot}$ (dashed lines). The black dots show the approximate position on the HR diagram of the binned averages of Figure 1, and the size of the dots is proportional to the Li abundance. The dotted lines show the location of stars with radii given by $R = 5,\ 10,\ 15,$ and $20\,R_{\odot}$.

As a further illustration of the relation between the stellar radius and the Li abundance, we have included in Figure 3 the average binned data from Figure 1, shown as black dots, where the luminosity was estimated from equation 2. The size of the dots is approximately proportional to the Li abundance, and the dotted lines show the location of stars with radius $R = 5,\ 10,\ 15,$ and $20\,R_{\odot}$. It can be seen that the stars with larger Li abundances, $\epsilon(\mathrm{Li}) \geq 3.0$, are closer to the location of the larger objects.

From the stellar mass and gravity, the stellar radius can be simply calculated as $R^2 = G\ M/g$, and the mass loss rate can be estimated by the Reimers formula

$$\frac{dM}{dt} = 4 \times 10^{-13}\ \eta\ \frac{(L/L_{\odot})\ (R/R_{\odot})}{(M/M_{\odot})} \qquad (3)$$

(see for example Lamers and Cassinelli 1999). The parameter η was originally considered as $\eta \leq 3$, but this calibration is probably not valid for the AGB/RGB stars considered here, so that we will consider it as a parameter to be determined.

4 Results and Discussion

The adopted value of the parameter η was obtained in the following way: As a first approximation, we adopt a linear relation between the mass loss rate $\log dM/dt$ and the luminosity $\log L/L_{\odot}$ for Li-rich stars of the form $\log dM/dt = e + f\ \log L/L_{\odot}$. The slope of this relation is then obtained using the Li-rich stars, and does not depend on the value of η. We obtain the following results: $f = 0.95 \pm 0.04$, with $n = 104$ and correlation coefficient $r = 0.91 \pm 0.42$.

Once the slope is fixed, we consider the Li-poor stars for which the mass loss rates and luminosities have been independently derived, which include the objects by Gullieuszik et al. (2012) and Groenewegen et al. (2009), with a total of 312 objects. We then use the total sample of 416 objects to determine the best value of the intercept e for the $\log dM/dt \times \log L/L_{\odot}$ correlation, that is, the intercept that corresponds to the slope derived for the Li-rich stars. This of course determines the parameter η, since for a given star the Reimers formula states that $dM/dt \propto \eta$. We have then for the whole sample of 416 stars the results: $\eta = 12.3$, $e = -10.34 \pm 0.16$, $f = 0.95 \pm 0.05$ with correlation coefficient $r = 0.72 \pm 1.03$.

The effectively used equation can be written as

$$\frac{dM}{dt} = 1.74 \times 10^{-12}\ \frac{10^{1.629\,\epsilon(\mathrm{Li})}}{(g\,M)^{1/2}} \qquad (4)$$

The mass loss rate dM/dt is in $M_{\odot}$/year, the Li abundance ϵ(Li) in dex, the gravity g in cm/s^2, and the stellar mass in solar masses. This equation is of the form $dM/dt = f[T_{eff}, g, \epsilon(\mathrm{Li})]$, since the mass depends on the effective temperature and on the luminosity, which is determined by the Li abundance.

Figure 4 shows the $\log dM/dt \times \log L/L_{\odot}$ plot including Li-rich stars (dots); Li-poor objects (Gullieuszik, stars; Groenewegen C-rich, empty circles; Groenewegen O-rich, empty triangles,).

We can make a rough estimate of the uncertainties involved in the determination of the mass loss rate by considering the typical uncertainties in the stellar properties adopted in this work. The uncertainty in the Li abundance ϵ(Li) is typically of 0.20 dex, according to the original sources cited in Section 2. The effective temperature T_{eff} is known to better than 100 K for most objects, and the gravity $\log g$ has a typical uncertainty of 0.20 dex. From the adopted correlations involving the stellar radius R and luminosity $\log L/L_{\odot}$, we would then expect average uncertainties of about $1\,R_{\odot}$ and 0.20 dex, respectively. This would translate into an uncertainty of about $0.5\,M_{\odot}$ for the solar mass, leading to a final uncertainty of about 0.50 dex for the mass loss rate $\log dM/dt$, which can also be estimated directly from figure 4. This is comparable with the uncertainties in the mass loss rates determined for Li-poor stars by Gullieuszik et al. (2012), which show an average dispersion of about 0.5 dex for $\log dM/dt$, corresponding roughly to a factor 2 for a typical mass loss rate of $dM/dt \sim 10^{-6}\,M_{\odot}$/year. Groenewegen et al. (2009) quote a slightly smaller uncertainty of 0.43 dex in $\log dM/dt$ for AGB stars and red supergiants in the Magellanic Clouds. It should be stressed, however, that our main point here is not the determination of the absolute value of the mass loss rate of Li-rich stars, but to compare their mass loss rates with those of most Li-poor giants.

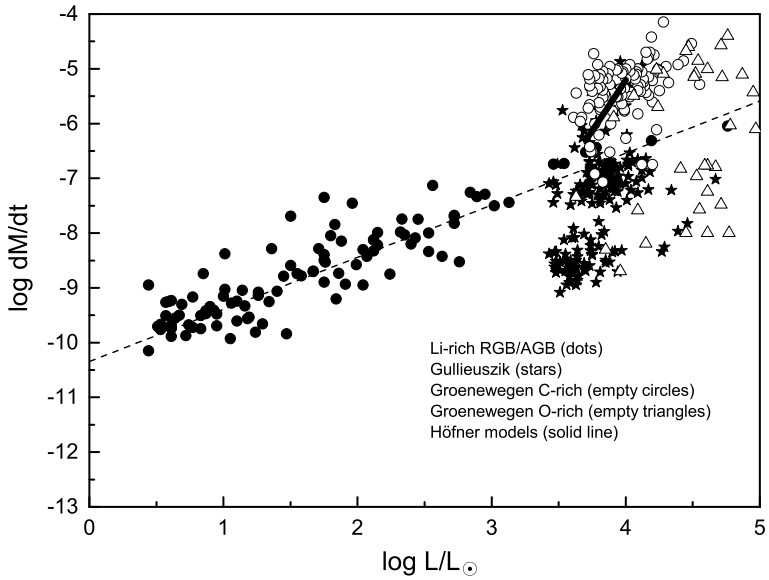

Figure 4: Luminosities and mass loss rates ($M_\odot$/year) for Li-rich stars (dots) and Li-poor stars (Gullieuszik, stars, Groenwegen C-rich, empty circles, Groenewegen O-rich, empty triangles, Höfner models, solid thick line.) The dashed line shows the derived linear relation.

Höfner & Andersen (2007) suggested a mass loss mechanism for M-type AGB stars based on the formation of carbon and silicate grains due to non-equilibrium effects. It is interesting to compare the results of these models with the present results, as shown in Figure 4. The model results can be approximately represented by average values of the luminosity and mass loss rates, which are included in the figure as a solid line. They are well placed in the upper right part of the diagram, where the O-rich giants are located, as expected. It can be seen that the agreement is fair, taking into account that the models apply to more luminous stars, having more intense mass loss rates than the Li-rich objects.

Li-enrichment has been associated with an enhanced mass loss ejection, as discussed by de La Reza et al. (1996, 1997). Monaco et al. (2011) comment that some Li-rich giants show evidences of mass loss and chromospheric activity, as discussed by Balachandran et al. (2000) and Drake et al. (2002). However, Fekel & Watson (1998) and Jasniewicz et al. (1999) suggested that no important mass loss phenomena are associated with these stars. By a comparison of K - [12 μm] colours of the 3 Li-rich stars with corresponding data for high mass loss Miras, Lebzelter et al. (2012) suggested that the Li-rich objects do not have enhanced dust mass loss. An enhanced gas mass loss has also been ruled out by the lack of asymmetries in the Ha profile, so that the conclusions by Fekel & Watson (1998) and Jasniewicz et al. (1999) are supported. In fact, as pointed out by Mallik (1999) and Luck (1977), a large amount of mass loss would remove the stellar outer layers where most Li atoms are located, so that strong mass loss rates are probably not associated with Li excess in AGB/RGB stars. The results shown in Figure 4 also confirm that the Li enrichment process does not seem to be associated with particularly strong mass loss rates, except for very high luminosity stars, which are a small fraction of the known Li-rich AGB/RGB stars.

Acknowledgments

This work was partially supported by FAPESP and CNPq.

References

Balachandran, S. C., Fekel, F. C., Henry, G. W., Uitenbroek, H. 2000, ApJ 542, 978

Bertelli, G., Girardi, L., Marigo, P., Nasi, E. 2008, A&A 484, 815

Brown, J. A., Sneden, C., Lambert, D. L., Dutchover, E. 1989, ApJ Suppl. 71, 293

Cameron, A. G. W., Fowler, W. A. 1971, ApJ 164, 111

Casey, A. R., Ruchti, G., Masseroni, T., et al. 2016, MNRAS 461, 3336

Charbonnel, C., Balachandran, S. C. 2000, A&A 359, 563

de La Reza, R., Drake, N. A., da Silva, L. 1996, ApJ 456, L115

de La Reza, R., Drake, N. A., da Silva, L., Torres, C. A. O., Martin, E. L. 1997, ApJ 482, L77

Delgado Mena, E., Tsantaki, et al. 2016a, Cool Stars 19, Uppsala

Delgado Mena, E., Tsantaki, M., et al. 2016b, A&A 587, A66

Drake, N. A., de la Reza, R., da Silva, L., Lambert, D. L. 2002, AJ 123, 2703

Fekel, F. C., Watson, L. C. 1998, AJ 116, 2466

Gonzalez, O. A., Zoccali, M., Monaco, L., Hill, V., Cassisi, S., Minniti, D., Renzini, A., Barbuy, B., Ortolani, S., Gomez, A. 2009, A&A 508, 289

Groenewegen, M. A. T., Sloan, G. C., Soszynski, I., Peterson, E. A. 2009, A&A 506, 1277

Groenewegen, M. A. T., Wood, P. R., Sloan, G. C., Blommaert, J. A. D. L., Cioni, M.-R. L., Feast, M. W., Hony, S., Matsuura, M., Menzies, J. W., Olivier, E. A., Vanhollebeke, E., van Loon, J. Th., Whitelock, P. A., Zijlstra, A. A., Habing, H. J., Lagadec, E. 2007, MNRAS 376, 313

Gullieuszik, M., Groenewegen, M. A. T., Cioni, M. R. L., de Grijs, R., van Loon, Th., Girardi, L., Ivanov, V. D., Oliveira, J. M., Emerson, J. P., Goardalini, R. 2012, A&A 537, A105

Höfner, S., Andersen, C. A. 2007, A&A 465, L39

Jasniewicz, G., Parthasarathy, M., de Laverny, P., Thévenin, F. 1999, A&A 342, 831

Kirby, E. N., Guhathakurta, P., Zhang, A. J., Hong, J., Guo, M., Guo, R., Cohen, J. G., Cunha, K. 2016, ApJ 819, 135

Kövári, Zs., Korhonen, H., Strassmeier, K. G., Weber, M., Kriskovics, L., Savanov, I. 2013, A&A 551, A2

Kumar, Y. B., Reddy, B. E., Lambert, D. L. 2011, ApJ 70, L12

Lamers, H. J. G. L., Cassinelli, J. 1999, Introduction to stellar winds, Cambridge

Lebzelter, T., Uttenthaler, S., Busso, M., Schultheis, M., Aringer, B. 2012, A&A 538, 36

Luck, R. E. 1977, ApJ 218, 752

Lyubimkov, L. S., Lambert, D. L., Kaminsky, B. M., Pavlenko, Y. V., Pokland, D. B., Rachkovskaya, T. 2012, MNRAS 427, 11

Maciel, W. J., Costa, R. D. D. 2012, Mem. S. A. It. S. 22, 103

Maciel, W. J., Costa, R. D. D. 2015, Why galaxies care about AGB stars III, ASP CS 497, 313

Mallik, S. V. 1999, A&A 352, 495

Martell, S. L., Shetrone, M. D. 2013, MNRAS 430, 611

Monaco, L., Villanova, S., Moni Bidin, C., Carraro, G., Geisler, D., Bonifacio, P., Gonzalez, O. A., Zoccali, M., Jilkova, L. 2011, A&A 529, A90

Monaco, L., Boffin, H. M. J., Bonifacio, P., Villanova, S., Carraro, G., Caffau, E., Steffen, M., Ahumada, J. A., Beletsky, Y., Beccari, G. 2014, A&A 564, L6

Vassiliadis, E., Wood, P. R. 1993, ApJ 413, 641

Wood, P. R., Bessell, M. S., Fox, H. W. 1983, ApJ 272, 99 33